*Environ. Sci. Technol.* **1999**, *33,* 1207−1212

# Influence of Chlorination on Chromophores and Fluorophores in Humic Substances

GREGORY V. KORSHIN,*,† MICHAEL U. KUMKE,‡ CHI-WANG LI,† AND FRITZ H. FRIMMEL‡

*Department of Civil and Environmental Engineering, University of Washington, Box 352700, Seattle, Washington 98195-2700, and Engler-Bunte-Institute, Water Chemistry Division, University of Karlsruhe, Richard-Wiltstätter-Allee 5, Karlsruhe 76131, Germany*

Three types of fluorophores (decay times 1.2, 4.3, and 10.7 ns, respectively) participate in the fluorescence of Suwannee River hydrophobic acid (HPOA). The emission of the fast-decaying fluorophores (FDF) is red-shifted compared with that of longer-decaying groups. Upon chlorination, the FDF contribution ($I_{FDF}$) to the emission declines, the specific absorbance at 254 nm ($SUVA_{254}$) decreases, and the electron-transfer absorbance band in the UV spectra of HPOA contracts. On the basis of the literature data and experimental evidence, the width of the electron-transfer absorbance band ($\Delta_{ET}$) is found to be proportional to the gyration radii ($R_g$) of the humic molecules. The $R_g$ values of chlorinated HPOA are also well-correlated with the energy of the emission band maximum ($E_{max}$) and emission bandwidth ($\Delta_{em}$). These consistent changes reflect the destruction of aromatic halogen attack sites accompanied by the breakdown of the humic molecules into smaller fragments.

## Introduction

Natural organic matter (NOM) is typically dominated by humic substances (HS), an operationally defined class of organic oligomers or polymers with molecular weights ranging from <1000 to >100000 Da (*1, 2, 3*). HS contain substantial amounts of hydroxy-, carboxy-, and methoxy-substituted aromatic units (*4, 5*) which are collectively referred to as polyhydroxyaromatic (PHA) or phenolic moieties. PHA is thought to constitute the substrate for halogenation reactions, and "masked" aromatic $\beta$-diketones (e.g., resorcinol, 3,5-dihydroxybezoic acids, and some flavonoids) are likely to be very important in the generation of trihalomethanes and possibly haloacetic acids (*6*−*9*).

The importance of activated aromatic, especially $\beta$-diketone, sites in the generation of trihalomethanes has been supported by experiments with model compounds (*7, 8, 10, 11*). However, efforts to probe the nature of the reaction sites in HS using structure-sensitive methods (notably, $^{13}C$ CP-MAS NMR), although successful (*12*−*14*), have had a limited scope. More insight into the nature of the reactive sites in NOM may be gained via in situ methods that use NOM concentrations typical for potable water (<10 mg/L of dissolved organic carbon, DOC), are structure-sensitive, provide information about the intermediates, and can be employed for a wide range of NOM types, pHs, and other reaction parameters.

UV absorbance and fluorescence of NOM meet several of these requirements, being simple, being sensitive to the presence of NOM, and possessing intrinsic, albeit complex, correlation with the internal structure of HS (*15*−*20*). Their use for NOM halogenation studies is attractive since the chromophores and fluorophores in NOM are activated aromatic units in PHA, and their involvement in halogenation may be tracked by both UV absorbance and fluorescence. Recent studies have shown a good correlation between the changes of UV absorbance spectra of NOM and formation of disinfection byproducts (*17, 21, 22*). The goal of this paper is to compare the effects of halogenation on the UV and fluorescence spectra of NOM and to explore their implications for understanding the halogenation mechanisms.

## Materials and Methods

The hydrophobic acids fraction (HPOA) from Suwannee River natural organic matter was used in all experiments. The samples were obtained by Jerry Leenheer at the U.S. Geological Survey Laboratory in Boulder, CO using the XAD-8 adsorption procedure (*23*) and contained <0.7% nitrogen and <0.3% sulfur. On the basis of $^{13}C$ CP-MAS NMR analysis (using a Chemagnetics CMX 200 MHz spectrometer at a spinning rate of 5000 Hz) aromatic and carboxylic groups accounted for approximately 26% and 22%, respectively, of the total carbon in the sample.

The experiments were conducted with samples containing 5.0 mg/L (as carbon) HPOA and 0.01 M $NaClO_4$. The dissolved organic carbon concentration was measured using an OI 700 carbon analyzer (OI Corp., College Station, TX). Chlorination was carried out at pH 7.0 and 25 °C, using Cl/DOC ratios from 0.1 to 4.0 mg/mg (with Cl expressed as $Cl_2$). Free chlorine was measured using the standard DPD-FAS titrimetric method (*24*). The reaction time was 7 days. No residual chlorine was present at the end of the exposure time. UV spectra were recorded with a Perkin-Elmer Lambda-18 dual-beam spectrophotometer. Instantaneous emission spectra were recorded with a Perkin-Elmer LS-50B fluorescence spectrometer using an excitation wavelength of 320 nm. Emission spectra were recorded from 360 to 560 nm at an angle of 90° versus the position of the excitation beam. The bandwidth of the slits was 5 nm. The fluorescence emission spectra were corrected for inner filter effect (*25*).

Time-resolved fluorescence measurements were performed using a FL900CDT fluorescence decay time spectrometer (Edinburgh Analytical Instruments) in the time-correlated single-photon counting mode. The instrument was set up in a T-geometry with two analyzing detection channels. A Hamamatsu R1527 photomultiplier tube (PMT) with a rise time of 2.2 ns was used for light detection. A nF900 nitrogen-filled nanosecond flash lamp (Edinburgh Analytical Instruments) operated at 40 kHz was used as the excitation light source. A Norland 5000 multichannel analyzer (MCA) (Viking Instruments Inc.) with a 4096-channels memory was operated in the pulse height analysis mode; 1024 channels of the MCA memory were attributed to each detection channel in a typical experiment. The stability of the excitation pulse profile was controlled throughout each fluorescence decay experiment. To obtain a sufficient number of counts in a wide dynamic range of the emitted light intensity, the measurements were done in cycles of 5000 counts. The counts from 10 cycles were summed to yield a

* Corresponding author: phone (206) 543-2394, fax: (206) 685-9185, e-mail: korshin@u.washington.edu.
† University of Washington.
‡ University of Karlsruhe.

10.1021/es980787h CCC: $18.00 
Published on Web 03/04/1999

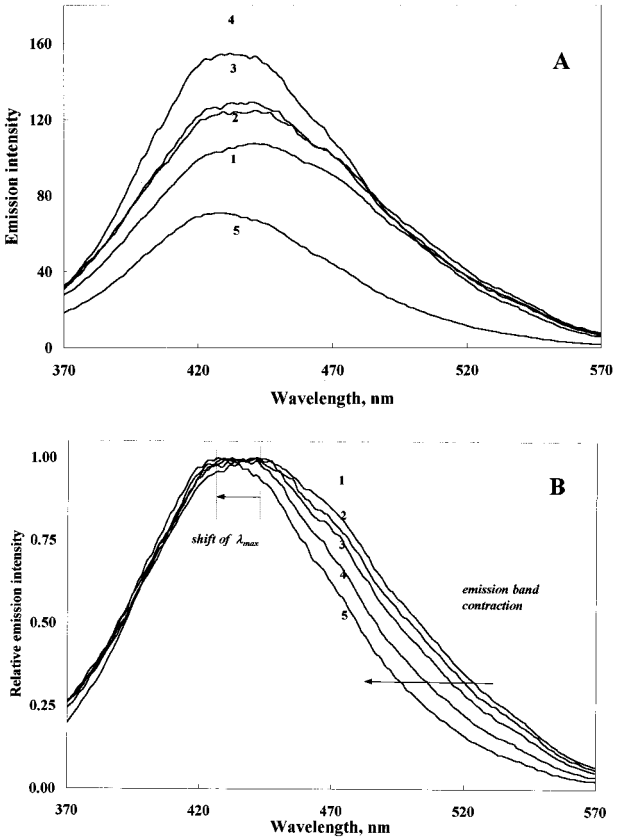


**FIGURE 1. Comparison of fluorescence emission spectra of chlorinated HPOA. Varying Cl/DOC ratios. DOC 5 mg/L. (1) 0 (initial sample); (2) 0.5; (3) 1.0; (4) 2.0; (5) 4.0. (A) Absolute intensities. (B) Normalized spectra.**

total of 50000 counts per emission decay profile in the maximum channel. The experiments were typically run at a time base of 100 ns with a 5 ns delay of the stop photomultiplier tube. The time calibration was 0.095 ns/channel. The excitation wavelength was 314 nm. The emitted light was monitored at 410 nm using a spectral bandwidth of 9 nm. To prevent counting artifacts caused by excessively high-photon loads, the counting rate was typically <1%, so pile-up problems in the decay time analysis were very unlikely. The instrument's software provided multiexponential data fitting, decay time distribution analysis, and global analysis. The experimental decay data were analyzed with nonlinear least-squares algorithms based on the Marquardt method. The results of the data-fitting procedures were evaluated using the $\chi^2$-values and the randomness of the weighed residuals. Only the fluorescence decay observed within the first 85 ns after the excitation flash was taken into account in the data fitting, and no shift term was introduced into the data analysis. The performance of our fluorescence decay time spectrometer was tested with a number of model compounds with known fluorescence decay times as described in ref *26*.

## Results

The fluorescence spectra of HPOA dosed with chlorine are shown in Figure 1A. The first 0.5 mg/L of chlorine had virtually no effect on the emission spectrum (data not shown), but subsequent Cl doses up to 10 mg/L caused the emission intensity to increase substantially.

When the spectra shown in Figure 1A are normalized by their respective maximum emission intensities, two trends are evident (Figure 1B): the position of the emission maximum ($\lambda_{max}$) exhibits a blue shift and the emission band contracts with increasing chlorine dose. To compare the shapes of the normalized spectra, the emission intensity was replotted as a function of the energy of the emitted light quanta ($E = 1240/\lambda$, where $E$ is the energy in eV and $\lambda$ is the wavelength in nm). The emission spectra were then fit using the Gaussian function (*27*):

$$I(E) = I_0 \exp\left[-\frac{4\ln(2)\,(E - E_{max})^2}{\Delta_{em}^{\,2}}\right] \qquad (1)$$

where $I_0$ and $E_{max}$ are the emission intensity ($I_0 = 1$ for normalized spectra) and the energy corresponding to the wavelength of maximum emission, respectively, and $\Delta_{em}$ is the width of the emission band measured at 50% of the maximum intensity.

**TABLE 1. Gauss Fitting Parameters for Emission Spectra of Chlorinated HPOA**

| Cl/DOC dose | $E_{max}$, eV | $\lambda_{max}$, nm | $\Delta_{em}$, eV |
|---|---|---|---|
| 0 | 2.82 | 440 | 0.69 |
| 0.1 | 2.82 | 440 | 0.69 |
| 0.5 | 2.83 | 438 | 0.68 |
| 0.8 | 2.84 | 437 | 0.67 |
| 1.0 | 2.85 | 435 | 0.65 |
| 2.0 | 2.86 | 434 | 0.61 |
| 4.0 | 2.89 | 429 | 0.58 |

The best-fit parameters and other data relevant for characterizing these samples according to eq 1 are given in Table 1. At Cl/DOC ≥ 0.5, halogenation affected both the position and the width of the Gauss band modeling the emission of HPOA. The emission bandwidth decreased from 0.69 eV in unchlorinated HPOA to 0.58 eV as the Cl/DOC ratio was increased to 4.0.

The Gauss function may be thought to describe the distribution of identical fluorophores in slightly different chemical environments associated with instantaneous conformational variations of polymeric/oligometic molecules of HS. The literature, however, indicates that HS contain more than one fluorophore-type (*28*−*32*) and the approximation of the emission or absorbance spectra using one Gauss band is not per se a proof of a one-fluorophore or one-chromophore model but a convenient way to quantify the influence of halogenation on the spectral bands. Manifestations of dissimilar fluorophores in the emission may also be detected using evolving factor analysis, by mathematical analysis of the spectra and by time-resolved spectroscopy that unambiguously evaluates the contribution of fluorophores with unequal decay times. The two latter approaches were used in this study.

The intrinsic structure of the emission spectra of HPOA and its chlorinated analogues was examined using the first-order derivatives of the normalized emission spectra (Figure 2A,B). The derivatives of all these spectra have structures that deviate from the one-band Gauss band model. These features were most evident for unaltered HPOA (Figure 2A). Their intensity substantially exceeded that of artifacts caused by high-frequency numerical noise in the spectra. Numerical processing using varying differentiation intervals (*27*) always resulted in the same features in the derivatives. These features (denoted as α, $\beta$, $\gamma$, and $\delta$ in Figure 2B) appear to indicate the presence of dissimilar chromophores.

The intersection of the derivatives with the abscissa shifts toward higher energy with increasing chlorine dose. This corresponds to the blue shift of the maximum of the emission spectra seen in the first-order emission data (e.g., Figure 1B). The intensity of feature $\gamma$ located at 2.61 eV is not affected by chlorination while that of feature $\delta$ steadily increases with the chlorine dose. In contrast, structures α and $\beta$ located at

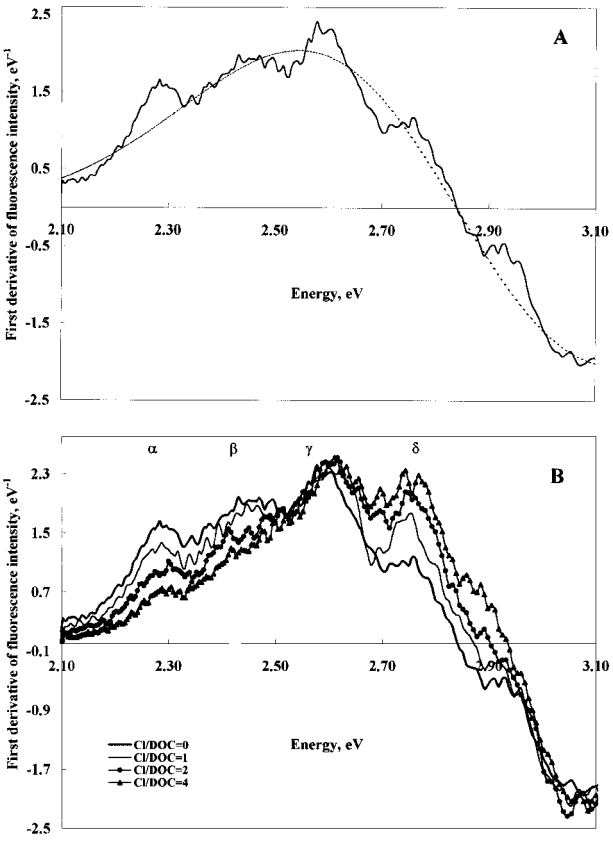


**FIGURE 2. First derivatives of selected normalized fluorescence emission spectra. (A) Comparison of the single-band Gauss fit with the experimental spectrum for unaltered HPOA and effects of minor bands. (B) First derivatives for varying chlorine/DOC ratios.**

2.29 and 2.45 eV become progressively weaker with the increase of the Cl/DOC ratio.

Time-resolved fluorescence confirmed the existence of dissimilar fluorophores in HPOA. The discrete component approach (DCA) which employs the smallest number of exponential terms to fit the observed decay was used to process the data. DCA analysis of the HPOA emission established that the emission decay profiles could be fitted using at least three exponential terms. To confirm the validity of the DCA approach, the fluorescence decay of HPOA was additionally evaluated using the distribution analysis, which does not introduce any a priori model of the fluorescence decay lifetimes distribution. These two methods of the evaluation of the fluorescence decay times are compared in more detail in refs *26, 33, 34*. It was found that the mean fluorescence decay times obtained using the distribution analysis mode were comparable to those calculated in the DCA mode. The trends observed for halogenated HPOA using either approach were identical. Therefore, only the DCA results will be discussed here. However, it needs to be recognized that the three fluorophores presumed to exist within the DCA approach are operationally defined and do not necessarily correspond to distinct chemical entities.

The contribution of the three components in the emission was evaluated presuming that the decay times of the three components were constant for all samples and only their relative contributions were affected by chlorination. The decay times were extracted having the goal of maximizing the global goodness-of-fit considering all the experimental data. The best-fit decay times (1.2, 4.3, and 10.7 ns) and the contributions of the respective fluorophores to the emission of chlorinated HPOA are shown in Table 2. The decay times shown are comparable with those reported for other HS

**TABLE 2. Fluorescence Decay Times Obtained for Chlorinated HPOA Samples; Emission Wavelength 410 nm**

| Cl/DOC dose | $\tau_1$ ($\sigma$), ns | $A_1$, % | $\tau_2$ ($\sigma$), ns | $A_2$, % | $\tau_3$ ($\sigma$), ns | $A_3$, % | $\xi^2$ |
|---|---|---|---|---|---|---|---|
| | | | Three Linked Exponential Terms | | | | |
| 0 | 1.2 (0.1) | 34.6 | 4.3 (0.3) | 45.9 | 10.7 (0.7) | 19.5 | 1.382 |
| 0.1 | | 36.8 | | 40.1 | | 23.1 | 1.388 |
| 0.8 | | 29.6 | | 41.2 | | 29.2 | 1.480 |
| 2.0 | | 29.5 | | 44.6 | | 25.9 | 1.352 |
| 4.0 | | 23.9 | | 51.0 | | 25.2 | 1.228 |

**TABLE 3. Parameters of UV Absorbance Spectra of Chlorinated HPOA**

| Cl/DOC dose | $SUVA_{254}$, L/(mg·m) | $A_{350}/A_{280}$ | $\Delta_{ET}$, eV |
|---|---|---|---|
| 0 | 5.01 | 0.413 | 2.31 |
| 0.1 | 4.90 | 0.416 | 2.32 |
| 0.5 | 4.54 | 0.393 | 2.25 |
| 0.8 | 4.19 | 0.377 | 2.20 |
| 1.0 | 4.07 | 0.366 | 2.17 |
| 2.0 | 3.21 | 0.319 | 2.04 |
| 4.0 | 1.85 | 0.208 | 1.74 |

samples (*28*−*32*). The respective fluorophores will be operationally referred to as the fast-, medium-, and slow-decaying fluorophores (FDF, MDF, and SDF, respectively).

The contribution of these fluorophores to the emission was affected by chlorination. For the unaltered sample, FDF, MDF, and SDF fluorophores contributed 35%, 46%, and 19% of the emission output, respectively. The lowest chlorine dose (Cl/DOC = 0.1) caused a marginal increase of the FDF and SDF contributions while that of MDF decreased correspondingly. A further increase of the chlorine dose reversed this trend. As the Cl/DOC ratio reached 4.0, the FDF contribution declined from 37% to 24% while those of the MDF and SFD increased from 40% to 51% and from 23% to 25%, respectively. Thus, the FDF sites are selectively eliminated by chlorination while the MDF and SDF contributions increase with the Cl dose.

Simultaneously with the changes in fluorescence, considerable effects in UV absorbance of HPOA were detected. Chlorination caused a substantial decrease of UV absorbance. Visually, the UV spectra of chlorinated HPOA were similar to those reported in refs *17, 21, 22*. The influence of chlorination on UV absorbance of HPOA was quantified based on the specific UV absorbance at 254 nm ($SUVA_{254}$), the ratio of absorbances at 280 and 350 nm ($A_{350}/A_{280}$), and the width of the electron-transfer band ($\Delta_{ET}$) (*17, 35*). The value of $\Delta_{ET}$ was calculated using the ratio of absorbances at 350 and 280 nm ($A_{350}/A_{280}$). Assuming that the Gaussian function (eq 1) can describe the shape of the ET band for $\lambda > 250$ nm and the maximum of the band is located in the range 252−254 nm (~4.90 eV) (*17, 35*), the following formula for $\Delta_{ET}$ was derived:

$$\Delta_{ET} = 2.18\left(\ln\left(\frac{A_{280}}{A_{350}}\right)\right)^{-1/2} \qquad (2)$$

The parameters of the UV spectra are compiled in Table 3. $SUVA_{254}$ has been reported to be proportional to the aromaticity of HS (*9*, *16*, 36, 37) although it may also be affected by nonaromatic conjugated double bonds. Accepting the position that $SUVA_{254}$ is mainly determined by the activated aromatic groups, its decrease from 5.01 to 1.85 L/(mg·m) seen in chlorinated HPOA supports the assumption that chlorine specifically targets these aromatic sites. The less anticipated effect is that the width of the ET band $\Delta_{ET}$

decreases from 2.31 to 1.74 eV as the Cl/DOC ratio increases. A possible meaning of $\Delta_{ET}$ for the chemistry of HS is discussed in the next section.

## Discussion

The trends in fluorescence and UV absorption spectra of chlorinated HPOA are summarized as follows:

(1) Chlorination causes the emission band to contract and shift toward lower $\lambda$ (higher quanta energies).

(2) The FDF contribution ($I_{FDF}$) to the fluorescence decreases with chlorine dose while that of MDF and SDF increases. This occurs simultaneously with the weakening of $\alpha$ and $\beta$ features and enhancement of the $\delta$ structure in the first derivatives of the emission spectra of HPOA.

(3) The intensity of fluorescence emission increases for a Cl/DOC ratio < 2.

(4) $SUVA_{254}$ and $\Delta_{ET}$ decrease.

We interpret these trends with the major premise that halogenation decreases the aromaticity of HPOA and causes its molecules to break down into smaller fragments. The literature establishes unambiguously that a decrease in the average molecular weight (AMW) of HS is associated with an increase of the fluorescence intensity (observed for Cl/DOC ratios < 2 in this work) (*38*−*41*). The reported time-resolved fluorescence data also indicate that the contribution of "medium" ($2 < \tau < 10$ ns) and "slow" ($\tau > 10$ ns) fluorophores increases with the decrease of AMW. This is accompanied by a decrease of the FDF contribution ($\tau < 2$ ns). For instance, HS with molecular weights 3−50 kDa have $I_{FDF}$ of 17% while for MW ranging from 50 to 100 kDa $I_{FDF}$ was 28% (*30*, *42*). The AMWs of aqueous HS are lower compared with that of soil HS, and the contribution of "medium" fluorophores in them is considerably higher (*43*).

We attempt to use the results of UV and fluorescence spectroscopy to probe the influence of halogenation on the size (deemed to be proportional to the AMW) of the HPOA molecules. We hypothesize that the width of the ET band may be indicative of the AMW of HS. The rationale for this assumption is that the chromophores in an HS molecule are more likely to interact each with other as the size of the molecule increases because of the increasing degree of conformational degrees of freedom. These interchromophore interactions may generate additional absorbance bands located at wavelengths longer than the ET bands of individual, noninteracting chromophores (*44*, *45*). If these bands are present, the single Gauss function employed for modeling the UV absorbance at $\lambda > 250$ nm should be viewed as a composite representation for a more complex system of overlapping bands. Because of their contribution, $\Delta_{ET}$ will increase with the AMW of HS.

The literature data allow testing this hypothesis. To do so, we used the published absorbance data at 254 and 400 nm for several humic and fulvic acids (*46*). This data set also contains the average sizes (giration radii, $R_g$) determined for the HS samples by low-angle X-ray diffraction. We calculated the corresponding $\Delta_{ET}$ for these samples and compared them to the reported radii. The $\Delta_{ET}$ values were calculated using a formula similar to formula 2 and presuming that the maximum of the ET band was located at 254 nm and the contribution of absorbance bands other than the ET band was negligible. The results are shown in Figure 3. A modest correlation between the radius of HS and $\Delta_{ET}$ was found for the series of 10 samples ($R^2 = 0.66$). The relationship between $\Delta_{ET}$ and $R_g$ was as follows:

$$R_E = 13.2\Delta_{ET} - 17.5 \quad (3)$$

where the giration radius is measured in Å and the width of the ET band is in eV. When one outlier was excluded, the correlation was much stronger ($R^2 = 0.78$). By contrast, the correlation between $R_g$ and $SUVA_{254}$ was weak ($R^2 = 0.33$). On the basis of these data, it was presumed that the changes of the giration radii of HPOA caused by halogenation might be semiquantitatively estimated using the $R_g$ versus $\Delta_{ET}$ correlation obtained for independent samples of HS. The giration radii of HPOA and its analogues calculated using formula 3 are estimates that need to be confirmed through independent experiments. It is nevertheless believed that the $R_g$ data so obtained allow evaluating the trends associated with HPOA halogenation.

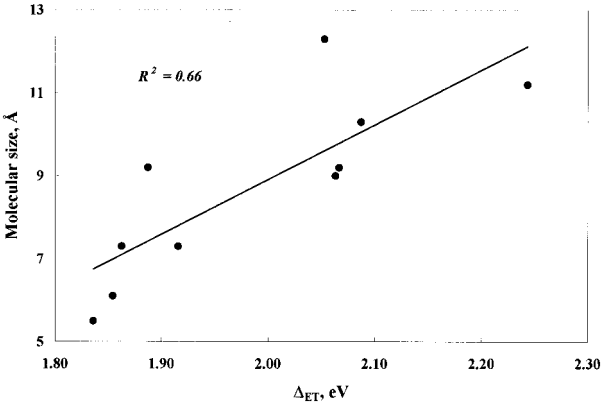


**FIGURE 3. Correlation between the giration radii and width of the electron-transfer band in HS. Data published in ref *46* are used for calculations.**

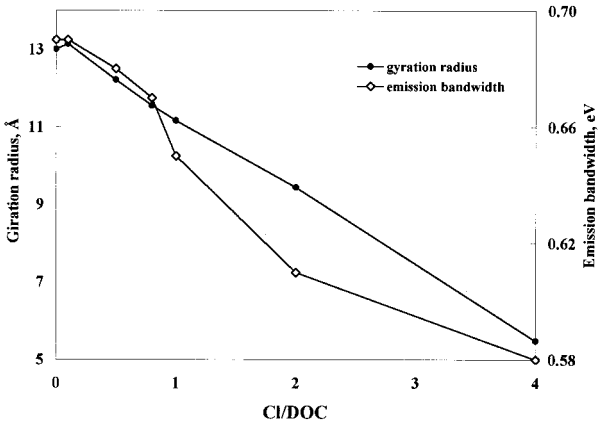


**FIGURE 4. Relationship between Cl/DOC dose and the giration radii and the width of emission of band of chlorinated HPOA.**

A good dose-property correlation between the Cl/DOC dose, the estimated giration radii of chlorinated HPOA, and the width of the emission band was found (Figure 4). For Cl/DOC > 0.1, the size of HPOA molecules decreases in parallel to the contraction of the fluorescence emission band. The giration radius of HPOA is also correlated with the position of the maximum in the emission spectra and with $I_{FDF}$. The correlation coefficients for these data sets are 0.89 and 0.97, respectively (Figure 5). The blue shift of the emission band and of the decrease of $I_{FDF}$ associated with the decrease of the molecular size demonstrated here corroborates the trends described qualitatively in the literature (*30*, *31*, *42*).

It has also been proposed that the fluorescence decay characteristics of HS may be affected by the energy transfer inside the polymeric molecules (*47*). In large HS molecules, intrafluorophore energy transfer shortens the apparent decay lifetimes of the fluorophores. In smaller molecules, this channel of the excitation energy dissipation may be weakened and the lifetimes of the fluorophores increase. Since chlorination decreases the size of the HPOA molecules and destroys some of the aromatic chromophores involved in

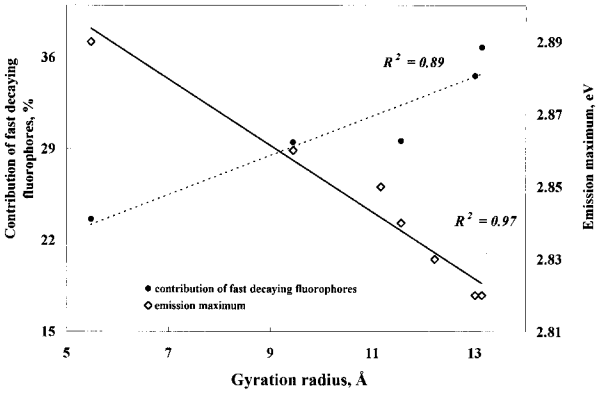


**FIGURE 5. Relationship between the estimated giration radii of halogenated HPOA, contribution of fast-decaying fluorophores ($\tau = 1.2$ ns) into the emission, and the position of maximum in the instantaneous emission spectra.**

the energy transfer, the decrease of $I_{FDF}$ in chlorinated HPOA correlates well with this hypothesis.

The blue shift of the emission associated with the depletion of FDF signifies that their contribution is more notable in the red part of the fluorescence spectra of HPOA. This is also demonstrated by the weakening of structures $\alpha$ and $\beta$ (located at 2.28 and 2.45 eV, respectively) in the derivatized emission spectra (Figure 2B). This indicates that the FDF emission band is likely to be located in the range of energy quanta from <2.5 to 2.6 eV ($\lambda$ > 480 nm). This location of emission spectra has been associated with high-AMW samples (e.g., humic acids extracted from soils and water sources (*19, 20, 41*)). The increase of the intensity of feature $\delta$ in chlorinated HPOA signifies that the emission of MDF and SDF is likely to be blue-shifted compared with that of FDF.

## Acknowledgments

The authors express their appreciation to Prof. Mark Benjamin (University of Washington, Seattle, WA) for his valuable critique. The authors thank Dr. Jerry Leenheer (U.S. Geological Survey, Denver, CO) who participated in the discussion of the results, provided, and characterized humic substances from Suwannee River, GA. This work was partly funded by the American Water Works Research Foundation (Project # 159-94). Support from HDR Engineering (Omaha, NE) is also greatly appreciated.

## Nomenclature

| | |
|---|---|
| AMW | average molecular weight |
| Cl/DOC | chlorine to DOC mass ratio |
| DCA | discrete component approach in the analysis of fluorescence decay |
| $\Delta_{ET}$ | width of the electron-transfer band in UV spectra, eV |
| $\Delta_{em}$ | width of the emission band in fluorescence spectra, eV |
| DOC | dissolved organic carbon, mg/L as carbon |
| $E_{max}$ | position of maximum in the emission spectra, eV |
| ET | electron transfer |
| eV | electron volt |
| FDF | fast-decaying fluorophores |
| HPOA | fraction of hydrophobic acids |
| HS | humic substances |
| $I_{FDF}$ | intensity of emission of fast-decaying fluorophores |
| MDF | medium-decaying fluorophores |
| NOM | natural organic matter |
| PHA | polyhydroxyaromatic moiety |
| $R_g$ | gyration radius |
| SDF | slow-decaying fluorophores |
| $SUVA_{254}$ | "specific" absorbance at 254 nm ($A_{254}$/DOC) |

## Literature Cited

(1) Thurman, E. M. *Organic Geochemistry of Natural Waters;* Nijhoff/Junk: Dordrecht, The Netherlands, 1985.
(2) Marinsky, J. A.; Reddy, M. M. *Chim. Acta* **1990**, *232*, 123−130.
(3) McIntyre, C.; Batts, B. D.; Jardine, D. R. *J. Mass Spectrom.* **1997**, *32*, 328−330.
(4) Stevenson, F. J. *Humus Chemistry, Genesis, Composition, Reactions, Spectroscopic Approaches*; Hayes, M. H. B., MacCarthy, P., Malcolm, R. L., Swift, R. L., Eds.; J. Wiley and Sons: New York, 1982; Chapter 11, pp 264−284.
(5) Christman, R. F.; Norwood, D. L.; Seo, Y.; Frimmel, F. H. Oxidative Degradation of Humic Substances from Freshwater Environments. In *Humic Substances II*; John Wiley & Sons: New York, 1989.
(6) Larson, R. A.; Weber, E. J. *Reaction Mechanisms in Environmental Organic Chemistry*; Lewis Publishers: Boca Raton, FL, 1994.
(7) Rook, J. J. *Environ. Sci. Technol.* **1977**, *11*, 478−482.
(8) Boyce, S. D.; Hornig, J. F. *Environ. Sci. Technol.* **1983**, *17*, 202−211.
(9) Reckhow, D. A.; Singer, P. C.; Malcolm, R. L. *Environ. Sci. Technol.* **1990**, *24*, 478−482.
(10) Topidurti, K. V.; Haas, C. N. *J. AWWA* **1991**, *83* (May), 62−66.
(11) Howard, A. G.; Pizzie, R. A.; Whitehouse, J. W. *Water Res.* **1985**, *19*, 241−248.
(12) Hanna, J. V.; Johnson, W. D.; Quezada, R. A.; Wilson, M. A.; Xia-Qiao, L. *Environ. Sci. Technol.* **1991**, *25*, 1160−1164.
(13) Thorn, K. A.; Arterburn, J. B.; Mikita, M. A. *Environ. Sci. Technol.* **1992**, *26*, 107−116.
(14) Ginwalla, A. S.; Mikita, M. A. *Environ. Sci. Technol.* **1992**, *26*, 1148−1150.
(15) Bloom, P. B.; Leenheer, J. A. Vibrational, Electronic and High-Energy Spectroscopic Methods for Characterizing Humic Substances. In *Humic Substances II*; Hayes, M. H. B., MacCarthy, P., Malcolm, R. L., Swift, R. L., Eds.; John Wiley & Sons: New York, 1989; pp 409−446.
(16) Chin, Y. P.; Aiken, G.; O'Loughlin, E. *Environ. Sci. Technol.* **1994**, *28*, 1853−1858.
(17) Korshin, G. V.; Li, C.-W.; Benjamin, M. M. *Water Res.* **1997**, *31*, 1787−1795.
(18) MacCarthy, P.; Rice, J. A. Spectroscopic Methods (Other than NMR) for Determining Functionality in Humic substances. In *Humic Substances in Soil, Sediment and Water*; Aiken, G. R., et al., Eds., John Wiley & Sons: New York, 1985.
(19) Senesi, N.; Miano, T.; Provenzano, M. R.; Brunetti, G. *Soil Sci.* **1991**, *152*, 259−271.
(20) Senesi, N. *Anal. Chim. Acta* **1990**, *232*, 77−106.
(21) Korshin, G. V.; Li, C.-W.; Benjamin, M. M. *Water Res.* **1997**, *34*, 946−949.
(22) Li, C.-W.; Korshin, G. V.; Benjamin, M. M. *J. AWWA* **1998**, *90* (Aug) 80−92.
(23) Leenheer, J. A. *Environ. Sci. Technol.* **1981**, *15*, 578−587.
(24) *Standard Methods for the Examination of Water and Wastewater*, 18th ed.; American Public Health Association, American Water Works Association, Water Pollution Control Federation: Washington, D. C., 1995.
(25) Puchalski, M. M.; Morra, M. J.; von Vandruska, R. *Fresenius J. Anal. Chem.* **1991**, *340*, 341−344.
(26) Frimmel, F. H.; Kumke, M. U. In *Humic Substances: Structure, Properties, and Uses*; Davies, G., Ghabbour, E.. Eds.; Royal Society of Chemistry: Cambridge, 1998; pp 113−122.
(27) Pelikán, P.; Ceppan, M.; Liška, M. *Application of Numerical Methods in Molecular Spectroscopy;* CRC Press: Boca Raton, FL, 1994.
(28) Goldberg, M. C.; Negomir, P. M. Characterization of Aquatic Humic Acid Fractions by Fluorescence Depolarization Spectroscopy. In *Luminescence Applications in Biological, Chemical, Environmental and Hydrological Sciences*; Goldberg, M. C., Ed.; ACS Symposium Series 383; American Chemical Society: Washington, D. C., 1989, pp 180−205.

(29) Gauthier, T. D.; Shane, E. C.; Guerin, W. F.; Seitz, W. R. *Environ. Sci. Technol.* **1986**, *20*, 1162−1166.
(30) Jones, G.; Indig, G. L. *New J. Chem.* **1996**, *20*, 221−232.
(31) Cook, R. L.; Lanford, C. H. *Anal. Chem.* **1995**, *67*, 174−180.
(32) McGown, L. B.; Hemmingsen, S. L.; Shaver, J. M.; Geng, L. *Appl. Spectrosc.* **1995**, *49*, 60−66.
(33) Tiseanu, C.; Kumke, M. U.; Frimmel, F. H.; Klenze, R.; Kim, J. I. *J. Photochem. Photobiol. A* **1998**, *117*, 175−184.
(34) Kumke, M. U.; Tiseanu, C.; Abbt-Braun, G.; Frimmel, F. H. *J. Fluoresc.* **1998**, *8*, 309−318.
(35) Korshin, G. V.; Li, C.-W.; Benjamin, M. M. Use of UV Spectroscopy to Study Chlorination of Natural Organic Matter. In *Water Disinfection and Natural Organic Matter;* Minear, R. A., Amy, G., Eds.; American Chemical Society: Washington, D.C., 1996.
(36) Traina, S. J.; Novak, J.; Smeck, N. E.; *J. Environ. Qual.* **1990**, *19*, 151−153.
(37) Edzwald, J. K.; Becker, W. C.; Wattier, K. L. *J. AWWA* **1985**, *77* (April), 122−132.
(38) Levesque, M. *Soil Sci.* **1972**, *113*, 346−353.
(39) Smart, P. L.; Finlayson, B. L.; Rylands, W. C.; Ball, C. M. *Water Res.* **1976**, *10*, 805−811.
(40) Stewart, A. J.; Wetzel, R. G. *Limnol. Oceanogr.* **1980**, *25*, 559−564.
(41) Hayase, K.; Tsubota, H. *Geochim. Cosmochim. Acta* **1985**, *49*, 159−163.
(42) Lochmueller, C. H.; Saavedra, S. S. *Anal. Chem.* **1986**, *58*, 1978−1981.
(43) Kumke, M. U.; Frimmel, F. H. *Proceedings of the 8th Meeting of the IHSS 8*, Wroclaw, Poland, Sept 9−14, 1996; Drozd, J., Gonet, S. S.; Senesi, N., Weber, J., Ed.; PTSH: Wroclaw, 1997; pp 525−531.
(44) Jaffe, H. H.; Orchin, M. *Theory and Applications of Ultraviolet Spectroscopy*; John Wiley and Sons: New York, 1962.
(45) Scott, A. I. *Interpretation of the Ultraviolet Spectra of Natural Products*. Pergamon Press: New York, 1964.
(46) Reckhow, D. A.; Singer, P. C.; Malcolm, R. L. *Environ. Sci. Technol.* **1990**, *24*, 1655−1664.
(47) Kumke, M. U.; Abbt-Braun, G.; Frimmel, F. H. *Acta Hydrochem. Hydrobiol.* **1998**, 73−81.

*Received for review July 31, 1998. Revised manuscript received January 13, 1999. Accepted January 19, 1999.*

ES980787H